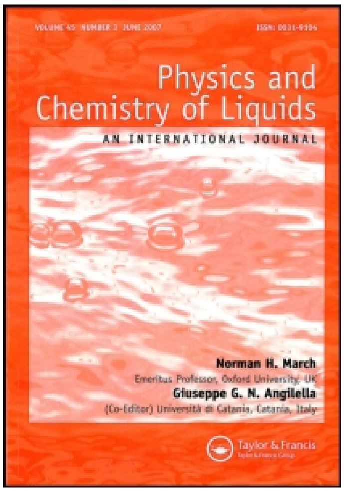

Physics and Chemistry of Liquids
Publication details, including instructions for authors and subscription information:
http://www.informaworld.com/smpp/title~content=t713646857

Thermodynamics of binary mixtures of aliphatic linear alkanes (C_6-C_{12}) at 298.15 K

A. Touriño[a]; M. Hervello[a]; V. Moreno[a]; M. Iglesias[a]; G. Marino[a]
[a] Laboratorio de Propiedades Fisicas, Centro de Apoyo Cientifico y Tecnológico a la Investigación (C.A.C.T.I.), Universidad de Vigo, 36200 Vigo, España

To cite this Article Touriño, A. , Hervello, M. , Moreno, V. , Iglesias, M. and Marino, G.(2004) 'Thermodynamics of binary mixtures of aliphatic linear alkanes (C_6-C_{12}) at 298.15 K', Physics and Chemistry of Liquids, 42: 1, 37 — 51
To link to this Article: DOI: 10.1080/0031910021000059054
URL: http://dx.doi.org/10.1080/0031910021000059054

Physics and Chemistry of Liquids
Vol. 42, No. 1, February 2004, pp. 37–51

THERMODYNAMICS OF BINARY MIXTURES OF ALIPHATIC LINEAR ALKANES (C_6–C_{12}) AT 298.15 K

A. TOURIÑO, M. HERVELLO, V. MORENO, M. IGLESIAS* and G. MARINO

Laboratorio de Propiedades Fisicas, Centro de Apoyo Cientifico y Tecnológico a la Investigación (C.A.C.T.I.), Universidad de Vigo, 36200 Vigo, España

(Received 12 June 2002)

This article reports experimental values of speeds of sound, densities and refractive indices on mixing of the binary mixtures *n*-hexane + (*n*-heptane, *n*-octane, *n*-nonane, *n*-decane, *n*-undecane, or *n*-dodecane) at 298.15 K and atmospheric pressure, over the whole concentration range. The corresponding excess and derived properties were computed from the experimental data. The results were fitted by means of the Redlich–Kister equation, such parameters being gathered. Different estimation methods (equations of state, mixing rules, Collision Factor and Free Length Theory) were applied, qualitative agreement between the experimental and theoretical values both in magnitude and sign being obtained.

Keywords: *n*-Alkane; Mixture; Density; Speed of sound; Refractive index

1. INTRODUCTION

Contamination of ground and surface water with halogenated, aromatic and aliphatic hydrocarbons is one of the different environmental problems mankind faces today. Recent legislation has resulted in continuously decreasing contaminating emissions, yet an important amount is still being emmitted to the environment. To this aim, an optimal design of separation units and development of freewaste processes and technologies are conditioned by an adequate knowledge of mixing thermodynamics, the estimation models playing an important role in the study and simulation of clean alternative unit operations.

The present work continues our research program on the chemical thermodynamics of mixtures related to pharmacological or chemical processes, as well as, in this case the identification and study of alternative separation agents and cosolvents in modified rectification processes [1–4]. In this way, the first step is the thermodynamic characterization of the mixtures (physical properties, vapor–liquid equilibria, liquid–liquid equilibria, etc) involved into the separation problem. In this article, we present new

---

*Corresponding author. Present address: Departament d'Enginyeria Química, Escola Tècnica Superìor d'Enginyeria Química, Universitat Rovira I Virgili, Avinguda Països Catalans 26, Campus Sescelades, 43007 Tarragona, España. Fax: + 34 977 559621. Email: maiglesias@etseq.urv.es

ISSN 0031-9104 print: ISSN 1029-0451 online © 2004 Taylor & Francis Ltd
DOI: 10.1080/0031910021000059054

measurements of different thermodynamic properties (speeds of sound, densities and refractive indices) of the binary mixtures *n*-hexane + (*n*-heptane, *n*-octane, *n*-nonane, *n*-decane, *n*-undecane, or *n*-dodecane) at 298.15 K, as well as, the corresponding derived magnitudes (changes of isentropic compressibilities on mixing, excess molar volumes and changes of refractive indices on mixing). In what is referred to the estimation of these magnitudes, different procedures were applied (equations of state for density, mixing rules for refractive indices and Free Length Theory/Collision Factor Theory for isentropic compressibilities), a qualitative agreement between the experimental and theoretical values both in magnitude and sign being obtained.

2. EXPERIMENTAL

All chemicals used were Merck chromatographic grade and were treated as usual in previous works [2]. Ultrasonic treatment was used for degassing and molecular sieves (type 4a or 3a, 1/16 in., Aldrich cat. n° 20.860-4 or 20.858-2, respectively) were introduced into the bottles to reduce possible water contents in solvents. The gas chromatographic analysis of pure components showed that the major peak area exceeds 99.0% for any solvent. Solution composition were determined gravimetrically, special care being taken during solution preparation to avoid evaporation losses. Further details of experimental procedure and mode of operation in our laboratory have been provided in earlier articles. The refractive indices of the pure liquids and mixtures were measured with the automatic refractometer ABBEMAT-HP Kernchen with a precision of $\pm 10^{-5}$ and thermostated with a PolyScience controller bath model 9010 with a temperature stability of $\pm 10^{-2}$ K. The densities and speeds of sound were measured with an Anton Paar DSA-48 digital densimeter and sound analizer with a precision of $\pm 10^{-4}\,\mathrm{g\,cm^{-3}}$ and $1\,\mathrm{m\,s^{-1}}$, respectively. Calibration of these apparatus was performed periodically, in accordance with technical specifications, using Millipore quality water (resistivity, 18.2 MΩ cm) and ambient air. A PolyScience controller bath model 9010 with a temperature stability of $\pm 10^{-2}$ K was used to thermostat the samples at least for 30 min. Samples were prepared by mass using a Mettler AT-261 Delta Range balance with an accuracy of $\pm 10^{-4}$ g, covering the whole composition ranges of the mixtures. The accuracy of the mole fractions, densities, refractive indices and speed of sound were estimated better than 10^{-4}, $2 \times 10^{-4}\,\mathrm{g\,cm^{-3}}$, 5×10^{-5} and $1\,\mathrm{m\,s^{-1}}$, respectively. Maximum deviation in the calculation of excess molar volumes, changes of refractive indices on mixing, and changes of isentropic compressibilities for these mixtures have been estimated better than $10^{-3}\,\mathrm{cm^3\,mol^{-1}}$, 10^{-4}, and $1\,\mathrm{TPa^{-1}}$, respectively. The values of the pure components, as well as, open literature data and contamination of water are enclosed into Table I.

3. DATA PROCEDURE

3.1. Correlation of Derived Magnitudes

The excess molar volumes, changes of refractive indices and changes of isentropic compressibilities on mixing values are presented in Table II and were computed from the

TABLE I GLC Purity. Maximum water content and comparison of data with literature for pure liquids at 298.15 K

Component	*Purity mass%*	*Max. water content mass%*	$\rho/(\mathrm{g\cdot cm^{-3}})$		n_D		$u/(\mathrm{m\cdot s^{-1}})$	
			Exptl.	*Lit.*[a]	*Exptl.*	*Lit*[a].	*Explt.*	*Lit.*
n-hexane	>99.2	$<7.8\times10^{-4}$	0.6551	0.65484 0.6549[b]	1.37234	1.37226	1077.0	1076.37[c]
n-heptane	>99.9	$<8.1\times10^{-4}$	0.6794	0.6794	1.38512	1.3850	1130.5	1131[d]
n-octane	>99.3	$<8\times10^{-4}$	0.6985	0.69862	1.39514	1.39505	1172.0	1180[e]
n-nonane	>99.2	$<2.6\times10^{-3}$	0.7142	0.71375	1.40336	1.40311	1207.35	1212[f]
n-decane	>99.6	$<10^{-3}$	0.7261	0.72614	1.40937	1.40967	1234.75	1234[e]
n-undecane	>99.0	$<10^{-3}$	0.7365	0.7365	1.41473	1.41507	1258.16	1257.95[g]
n-dodecane	>99.6	$<10^{-3}$	0.7451	0.74518	1.41953	1.41949	1279.61	1277.97[g]

[a][5]; [b][6]; [c][7]; [d][8]; [e][9]; [f][10]; [g][11].

TABLE II Densities ρ, refractive indices n_D, speeds of sound u, isentropic compressibilities κ_s, excess molar volumes V^E, changes of refractive indices δn_D and changes of isentropic compressibilities $\delta\kappa_s$ for the binary mixtures *n*-hexane + (*n*-heptane, *n*-octane, *n*-nonane, *n*-decane, *n*-undecane, or *n*-dodecane) at 298.15 K

X	$\rho/(\mathrm{g\,cm^{-3}})$	n_D	$u/(\mathrm{m\,s^{-1}})$	$\kappa_s/(\mathrm{TPa^{-1}})$	$V^E/(\mathrm{cm^3\,mol^{-1}})$	δn_D	$\delta\kappa_s/(\mathrm{TPa^{-1}})$
n-hexane + *n*-heptane							
0.0509	0.6783	1.38450	1127.8	1159.2	0.00014	0.00023	−0.8
0.1066	0.6771	1.38390	1124.8	1167.4	0.00027	0.00034	−1.8
0.1898	0.6752	1.38293	1120.5	1179.7	0.00039	0.00042	−3.1
0.3182	0.6722	1.38140	1114.1	1198.5	0.00053	0.00051	−5.4
0.4190	0.6698	1.38016	1109.0	1213.9	0.00060	0.00055	−6.6
0.5269	0.6672	1.37880	1103.7	1230.3	0.00064	0.00055	−7.9
0.5987	0.6655	1.37788	1100.2	1241.4	0.00065	0.00054	−8.7
0.6993	0.6630	1.37655	1095.2	1257.5	0.00059	0.00048	−9.1
0.7995	0.6605	1.37520	1089.6	1275.5	0.00048	0.00040	−7.6
0.9081	0.6577	1.37370	1082.8	1296.9	0.00032	0.00027	−4.0
0.9587	0.6563	1.37296	1079.7	1307.1	0.00019	0.00017	−2.1
n-hexane + *n*-octane							
0.0452	0.6970	1.39442	1167.9	1051.9	−0.00515	0.00031	−2.7
0.0954	0.6953	1.39332	1164.5	1060.7	−0.02346	0.00035	−7.6
0.1910	0.6919	1.39168	1157.3	1079.2	−0.04879	0.00089	−15.3
0.2908	0.6881	1.38974	1148.8	1101.2	−0.07437	0.00123	−20.6
0,4064	0.6836	1.38734	1138.3	1129.2	−0.09228	0.00146	−24.3
0.4912	0.6801	1.38549	1130.8	1150.1	−0.09867	0.00155	−26.6
0.5975	0.6755	1.38307	1120.7	1178.9	−0.10872	0.00155	−26.9
0.6985	0.6708	1.38071	1110.7	1208.6	−0.09732	0.00149	−24.8
0.7982	0.6659	1.37808	1099.8	1241.6	−0.07559	0.00114	−19.2
0.9014	0.6606	1.37523	1088.2	1278.6	−0.03992	0.00064	−10.4
0.9504	0.6579	1.37383	1083.0	1296.1	−0.01408	0.00036	−6.3
n-hexane + *n*-nonane							
0.0469	0.7120	1.40218	1203.0	970.5	0.0353	0.00028	−7.6
0.0957	0.7100	1.40112	1198.2	981.0	−0.0127	0.00073	−14.4
0.2165	0.7045	1.39828	1185.8	1009.5	−0.0592	0.00163	−28.7
0.2983	0.7005	1.39632	1177.2	1030.1	−0.0785	0.00221	−37.1
0.4005	0.6953	1.39365	1165.1	1059.5	−0.1196	0.00271	−44.0
0.5238	0.6885	1.39022	1149.8	1098.6	−0.1500	0.00311	−48.5
0.5940	0.6844	1.38804	1140.5	1123.3	−0.1706	0.00311	−48.8
0.7006	0.6775	1.38445	1126.2	1163.7	−0.1351	0.00282	−46.1
0.8013	0.6707	1.38088	1111.0	1207.9	−0.1374	0.00238	−37.7

(*continued*)

TABLE II Continued

X	$\rho/(\mathrm{g\,cm^{-3}})$	n_D	$u/(\mathrm{m\,s^{-1}})$	$\kappa_s/(\mathrm{TPa^{-1}})$	$V^E/(\mathrm{cm^3\,mol^{-1}})$	δn_D	$\delta\kappa_s/(\mathrm{TPa^{-1}})$
0.9035	0.6631	1.37680	1094.7	1258.5	−0.0978	0.00146	−23.3
0.9516	0.6591	1.37466	1086.4	1285.5	−0.0324	0.00082	−13.4
n-hexane + *n*-decane							
0.0462	0.7239	1.40829	1229.6	913.6	−0.00954	0.00063	−9.2
0.0967	0.7215	1.40728	1223.2	926.4	−0.04184	0.00149	−17.3
0.1966	0.7165	1.40485	1211.9	950.3	−0.10641	0.00276	−34.6
0.2976	0.7110	1.40201	1200.3	976.2	−0.15426	0.00366	−50.2
0.4000	0.7049	1.39892	1185.3	1009.8	−0.18113	0.00436	−58.9
0.5005	0.6984	1.39557	1171.5	1043.1	−0.22276	0.00473	−67.0
0.6060	0.6911	1.39160	1154.7	1085.3	−0.24207	0.00467	−68.3
0.6919	0.6843	1.38800	1140.2	1123.9	−0.21726	0.00425	−65.1
0.8037	0.6750	1.38303	1120.2	1180.7	−0.18334	0.00342	−54.4
0.9029	0.6655	1.37793	1099.5	1242.9	−0.12441	0.00200	−33.1
0.9509	0.6605	1.37536	1089.1	1276.4	−0.06675	0.00120	−19.4
n-hexane + *n*-undecane							
0.0471	0.7343	1.41388	1253.9	869.6	−0.03334	0.00114	−13.0
0.0946	0.7319	1.41275	1248.3	880.4	−0.09808	0.00203	−24.2
0.1944	0.7266	1.40987	1235.4	905.2	−0.18745	0.00338	−45.1
0.2997	0.7206	1.40695	1221.4	933.9	−0.27802	0.00490	−64.7
0.3913	0.7147	1.40382	1207.6	963.1	−0.35185	0.00568	−77.6
0.5019	0.7069	1.39982	1189.3	1004.0	−0.38682	0.00636	−87.4
0.6023	0.6989	1.39578	1171.5	1046.6	−0.40095	0.00658	−91.0
0.7030	0.6898	1.39102	1151.2	1098.1	−0.36169	0.00609	−85.8
0.8027	0.6798	1.38556	1129.5	1157.3	−0.32257	0.00486	−72.3
0.9013	0.6682	1.37942	1105.2	1229.4	−0.18307	0.00290	−45.6
0.9503	0.6620	1.37604	1092.0	1271.2	−0.09479	0.00159	−26.3
n-hexane + *n*-dodecane							
0.0450	0.7430	1.41821	1273.0	830.5	−0.08353	0.00080	−12.7
0.0985	0.7403	1.41677	1266.5	842.1	−0.15435	0.00189	−27.6
0.1935	0.7350	1.41424	1253.4	866.0	−0.23319	0.00384	−50.8
0.3009	0.7283	1.41084	1237.7	896.3	−0.29229	0.00551	−73.7
0.3986	0.7216	1.40735	1221.7	928.4	−0.35519	0.00663	−89.9
0.5014	0.7137	1.40335	1203.4	967.5	−0.40129	0.00748	−101.6
0.6140	0.7038	1.39801	1180.7	1019.2	−0.41007	0.00745	−105.7
0.7124	0.6938	1.39275	1157.8	1075.1	−0.36647	0.00684	−98.5
0.8022	0.6835	1.38718	1134.5	1136.7	−0.30975	0.00551	−81.4
0.9050	0.6699	1.38013	1106.8	1218.6	−0.19098	0.00330	−50.3
0.9520	0.6628	1.37664	1091.1	1267.4	−0.09160	0.00203	−24.8

Eqs. (1)–(3):

$$V^E = \sum_{i=1}^{n} x_i M_i(\rho^{-1} - \rho_i^{-1}), \tag{1}$$

$$\delta n_D = n_D - \sum_{i=1}^{n} x_i n_{Di}, \tag{2}$$

$$\delta_{k_s} = \frac{1}{\rho u^2} - \sum_{i=1}^{n} \frac{x_i}{\rho_i u_i^2}, \tag{3}$$

In these equations, ρ is the density, n_D the refractive index on mixing and κ_s the isentropic compressibility on mixing. The ρ_i, n_{Di} and κ_{si} symbols are the properties of

TABLE III Fitting parameters of Eq. (4) and root mean square deviations (σ)

n-hexane + *n*-heptane				
$V^E/(\mathrm{cm^3\,mol^{-1}})$	$B_0 = 2{,}029817 \times 10^{-3}$	$B_1 = 8{,}803189 \times 10^{-5}$		$\sigma = 7 \times 10^{-6}$
δn_D	$B_0 = 2{,}137728 \times 10^{-3}$	$B_1 = -2{,}072004 \times 10^{-4}$	$B_2 = 1{,}754686 \times 10^{-3}$	$\sigma = 3 \times 10^{-5}$
$\delta\kappa_s/(\mathrm{TPa^{-1}})$	$B_0 = -2{,}977079 \times 10^{1}$	$B_1 = -2{,}328337 \times 10^{1}$	$B_2 = -1{,}660125$	
	$B_3 = 7{,}555595$	$B_4 = 2{,}147416 \times 10^{1}$		$\sigma = 10^{-1}$
n-hexane + *n*-octane				
$V^E/(\mathrm{cm^3\,mol^{-1}})$	$B_0 = -4{,}181857 \times 10^{-1}$	$B_1 = -1{,}238210 \times 10^{-1}$	$B_2 = 9{,}740896 \times 10^{-2}$	$\sigma = 4 \times 10^{-3}$
δn_D	$B_0 = 6{,}310293 \times 10^{-3}$	$B_1 = 1{,}332047 \times 10^{-3}$		$\sigma = 5 \times 10^{-5}$
$\delta\kappa_s/(\mathrm{TPa^{-1}})$	$B_0 = -1{,}073841 \times 10^{2}$	$B_1 = -2{,}103217 \times 10^{1}$	$B_2 = 1{,}253912$	$\sigma = 6 \times 10^{-1}$
n-hexane + *n*-nonane				
$V^E/(\mathrm{cm^3\,mol^{-1}})$	$B_0 = -6{,}002244 \times 10^{-1}$	$B_1 = -5{,}125213 \times 10^{-1}$		$\sigma = 8 \times 10^{-3}$
δn_D	$B_0 = 1{,}214835 \times 10^{-2}$	$B_1 = 4{,}481593 \times 10^{-3}$		$\sigma = 5 \times 10^{-5}$
$\delta\kappa_s/(\mathrm{TPa^{-1}})$	$B_0 = -1{,}917866 \times 10^{2}$	$B_1 = -4{,}925136 \times 10^{1}$	$B_2 = -3{,}547347 \times 10^{1}$	
	$B_3 = -2{,}251029 \times 10^{1}$			$\sigma = 3 \times 10^{-1}$
n-hexane + *n*-decane				
$V^E/(\mathrm{cm^3\,mol^{-1}})$	$B_0 = -8{,}913850 \times 10^{-1}$	$B_1 = -4{,}648187 \times 10^{-1}$		$\sigma = 8 \times 10^{-3}$
δn_D	$B_0 = 1{,}878304 \times 10^{-2}$	$B_1 = 3{,}480428 \times 10^{-3}$	$B_2 = 1{,}952959 \times 10^{-3}$	$\sigma = 7 \times 10^{-5}$
$\delta\kappa_s/(\mathrm{TPa^{-1}})$	$B_0 = -2{,}656929 \times 10^{2}$	$B_1 = -8{,}502628 \times 10^{1}$	$B_2 = -4{,}297311 \times 10^{1}$	
	$B_3 = -4{,}027931 \times 10^{1}$			$\sigma = 7 \times 10^{-1}$
n-hexane + *n*-undecane				
$V^E/(\mathrm{cm^3\,mol^{-1}})$	$B_0 = -1{,}572632$	$B_1 = -6{,}291485 \times 10^{-1}$	$B_2 = 9{,}137845 \times 10^{-3}$	$\sigma = 8 \times 10^{-3}$
δn_D	$B_0 = 2{,}564131 \times 10^{-2}$	$B_1 = 8{,}464418 \times 10^{-3}$	$B_2 = 9{,}867478 \times 10^{-4}$	
	$B_3 = -4{,}130438 \times 10^{-3}$	$B_4 = 4{,}037822 \times 10^{-3}$		$\sigma = 7 \times 10^{-5}$
$\delta\kappa_s/(\mathrm{TPa^{-1}})$	$B_0 = -3{,}365192 \times 10^{2}$	$B_1 = -1{,}243632 \times 10^{2}$	$B_2 = -2{,}663656 \times 10^{1}$	
	$B_3 = -2{,}259479 \times 10^{1}$			$\sigma = 5 \times 10^{-1}$
n-hexane + *n*-dodecane				
$V^E/(\mathrm{cm^3\,mol^{-1}})$	$B_0 = -1{,}562613$	$B_1 = -5{,}762453 \times 10^{-1}$	$B_2 = -4{,}785099 \times 10^{-1}$	
	$B_3 = 5{,}217193 \times 10^{-1}$			$\sigma = 9 \times 10^{-3}$
δn_D	$B_0 = 2{,}964567 \times 10^{-2}$	$B_1 = 9{,}241535 \times 10^{-3}$		$\sigma = 10^{-4}$
$\delta\kappa_s/(\mathrm{TPa^{-1}})$	$B_0 = -4{,}023431 \times 10^{2}$	$B_1 = -1{,}579736 \times 10^{2}$	$B_2 = -3{,}787695 \times 10^{1}$	
	$B_3 = -1{,}274232 \times 10^{1}$			$\sigma = 9 \times 10^{-1}$

pure chemicals and n is the number of components in the mixture. A Redlich–Kister [12] type equation was used to correlate the derived properties of the binary mixtures, by using the unweighted least squares method, all experimental points weighting equally. The Redlich–Kister equation can be expressed as:

$$\delta Q = x_i x_j \cdot \sum_{\rho=0}^{m} B_p (x_i - x_j)^p, \tag{4}$$

where δQ is $V^E/(\mathrm{cm^3\,mol^{-1}})$, δn_D or $\delta\kappa_s/(\mathrm{TPa^{-1}})$, respectively. The degree of this equation (m parameter) was optimized by applying the F-test [13]. The fitting parameters are gathered into Table III, with the corresponding root mean square deviations. Only previously published data have been found in open literature for the excess molar volumes and changes of refractive indices at the studied conditions of some of the mixtures. Figures 1–3 show the derived properties plotted against x_1 (*n*-hexane), as well as the curves fitted by Eq. (4). Almost the whole mixtures show a contractive trend at any composition, due to the dispersive interactions that reach a maximum for approximately equimolar mixtures and rising molar weight of the diluent of *n*-hexane. As an exception providing the tendence, the mixture *n*-hexane + *n*-heptane shows a negligible tendence (minor than $5 \times 10^{-3}\,\mathrm{cm^3\,mol^{-1}}$) of slight expansion at any molar fraction of *n*-hexane. The tendence of this mixture at the same temperature was

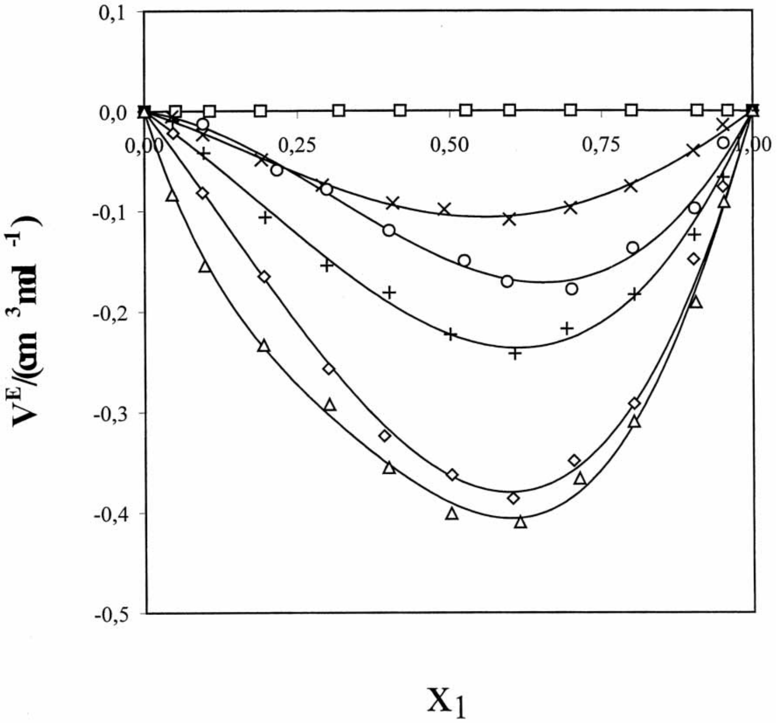

FIGURE 1 Dependence of excess molar volumes ($cm^3\ mol^{-1}$) with mole fraction at 298.15 K for *n*-hexane + , ((□) *n*-heptane, (×) *n*-octane, (○) *n*-nonane, (+) *n*-decane, (◇) *n*-undecane, or (Δ) *n*-dodecane) and (—, Eq. (4)) fitting curves.

gathered as slightly contractive [14,15] or sigmoidal [16] in previous works, which contrasts with the obtained measurements. Due to the discrepancy between previously measurements and our results, the final reported data for *n*-hexane + *n*-heptane were repeated with careful attention, the same behavior being observed. The trend of the excess molar volumes are in accordance with the temperature dependence presented in a recent work developed in our laboratory [17]. The deviations from earlier published data should be observed in Fig. 4(a–d). In these figures, the deviations of the excess molar [14–16], and those corresponding to changes of refractive indices [16] from literature are showed (Fig. 4(d)). The deviations corresponding to the excess molar volumes are lower than 5% with the exception of *n*-hexane + *n*-heptane mixture where are higher than 50%. No values were found for isentropic compressibilities in open literature. It could be observed as the deviations of changes of refractive index show deviations around 3–5% at any composition.

3.2. Partial Excess Molar Volumes

Partial molar quantities are important in the study of the dependence of an extensive property on the phase composition at constant pressure and temperature, because show its trend with molar fraction variation. They should be applied to any extensive property of a single-phase system such as volume, Gibbs energy or any other. If we let

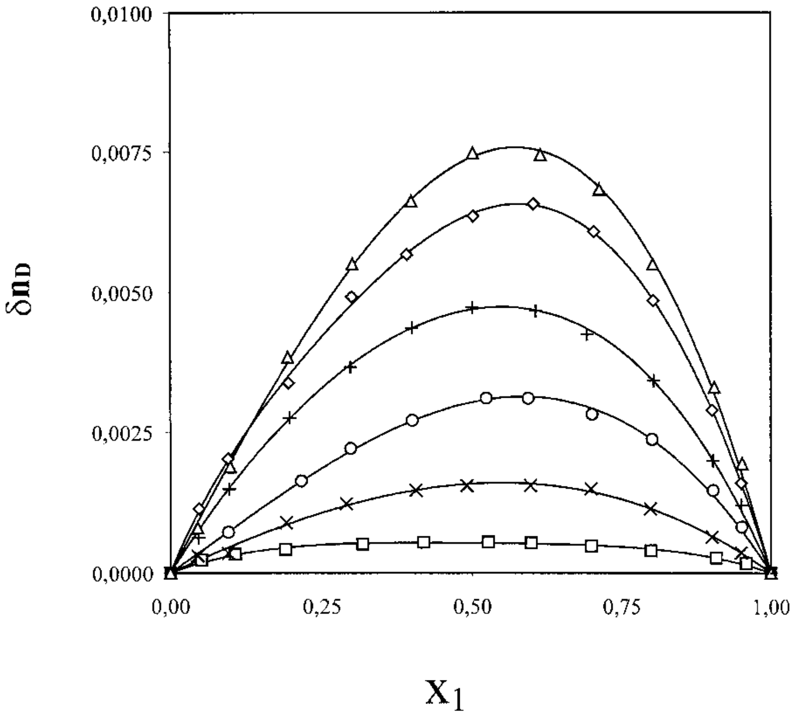

FIGURE 2 Dependence of change of refractive indices with mole fraction at 298.15 K for *n*-hexane + ((□) *n*-heptane, (×) *n*-octane, (○) *n*-nonane, (+) *n*-decane, (◇) *n*-undecane, or (Δ) *n*-dodecane) and (—, Eq. (4)) fitting curves.

E represent any extensive property of a single phase which is a function of pressure, temperature and mole numbers of the components, the differential of E should be expressed as:

$$\delta E = \left(\frac{\partial E}{\partial T}\right)_{P,n} dT + \left(\frac{\partial E}{\partial P}\right)_{T,n} dP + \sum_{i=1}^{N} \left(\frac{\partial E}{\partial n_i}\right)_{T,P,n} dn_i \tag{5}$$

where the quantity $(\partial E/\partial n_i)_{T,P,n}$ is defined as the partial molar quantity of the ith component in the phase, the value n refers to all the other components present, showing the finite change in the property on the addition of 1 mol of the component i in an infinite quantity of solution at constant temperature and pressure. In what is referred to as an excess property, the partial excess molar volume of a component in a binary mixture can be determined from excess molar volume data taking into account we have applied the Redlich–Kister expression to fit the excess values, thus the parameters enclosed in Table III for Eq. (4) are applied. The expression for the partial excess molar volume, should be written as:

$$\overline{V}_i^E = (1 - x_i)^2 \left[\sum_{p=0}^{m} B_p (2x_1 - 1)^p + x_i \sum_{p=1}^{m} (-2)^{i-1} p B_p (2x_1 - 1)^{p-1} \right] \tag{6}$$

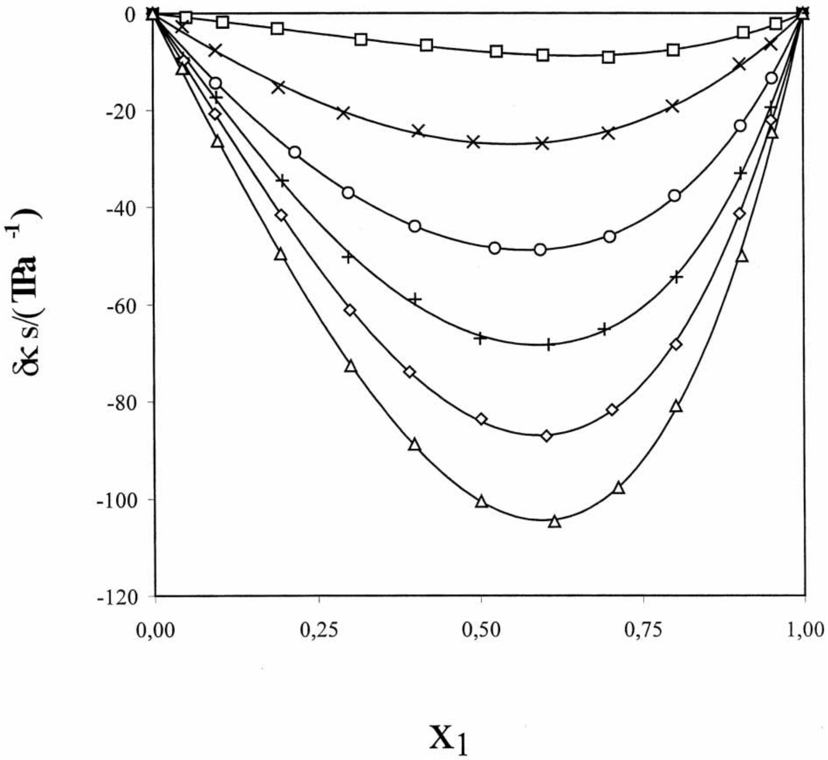

FIGURE 3 Dependence of change of isentropic compressibilities (TPa^{-1}) with mole fraction at 298.15 K for *n*-hexane + ((□) *n*-heptane, (×) *n*-octane, (○) *n*-nonane, (+) *n*-decane, (◇) *n*-undecane, or (Δ) *n*-dodecane) and (—–, Eq. (4)) fitting curves.

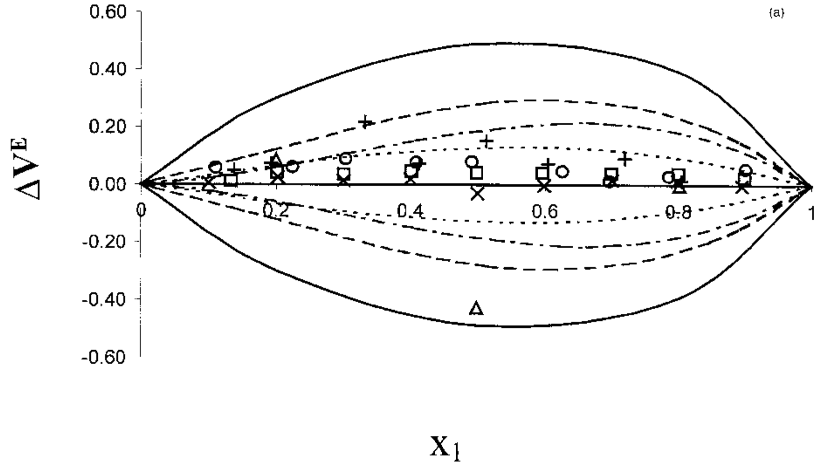

FIGURE 4 Deviations for *n*-hexane + ((□) *n*-heptane, (×) *n*-octane, (○) *n*-nonane, (+) *n*-decane, or (Δ) *n*-dodecane) from the open literature references (a) [14], (b) [15], (c) [16] and (d) [16]. The lines show deviations from our experimental data (ΔV^E, Figs. 4(a–c) for *n*-hexane + ((···) *n*-heptane (±50%), (- - -) *n*-octane (±5%), (–··–) *n*-nonane (±5%), (— —) *n*-decane (±5%), (···) *n*-dodecane (±5%), $\Delta\delta n_D$ for *n*-hexane + ((···) *n*-heptane, (—) *n*-octane, (–·–) *n*-nonane, (– –) *n*-decane, (—–) *n*-dodecane (±10% for all cases)).

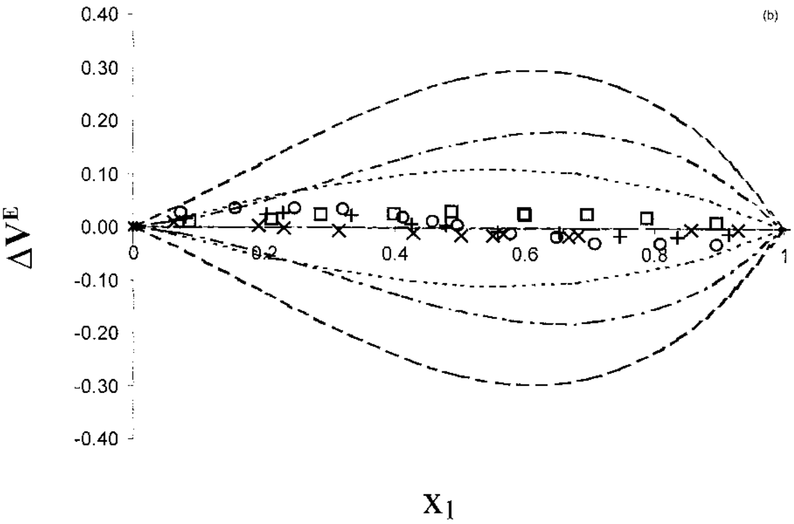

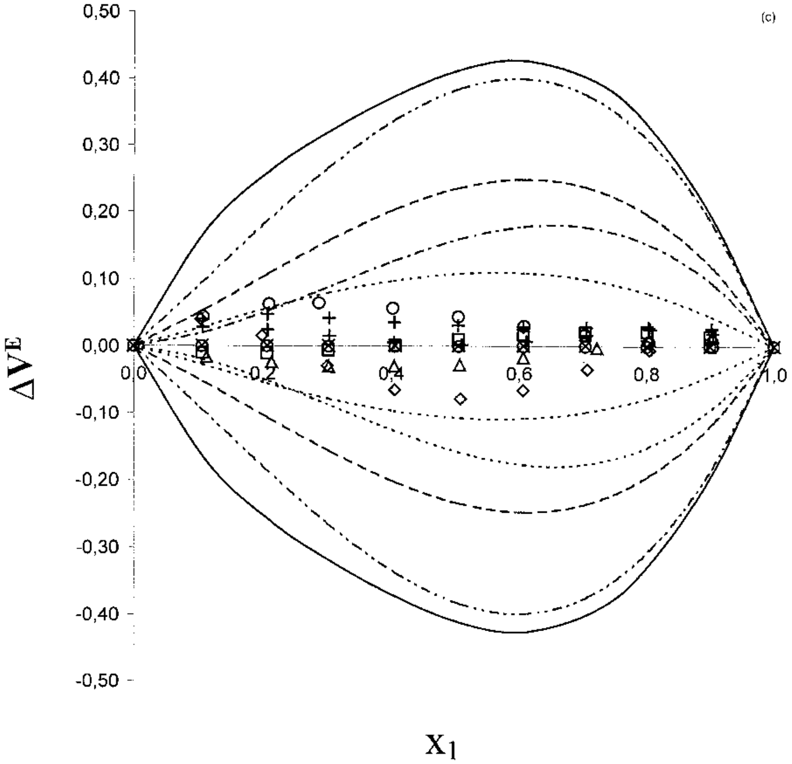

FIGURE 4 Continued.

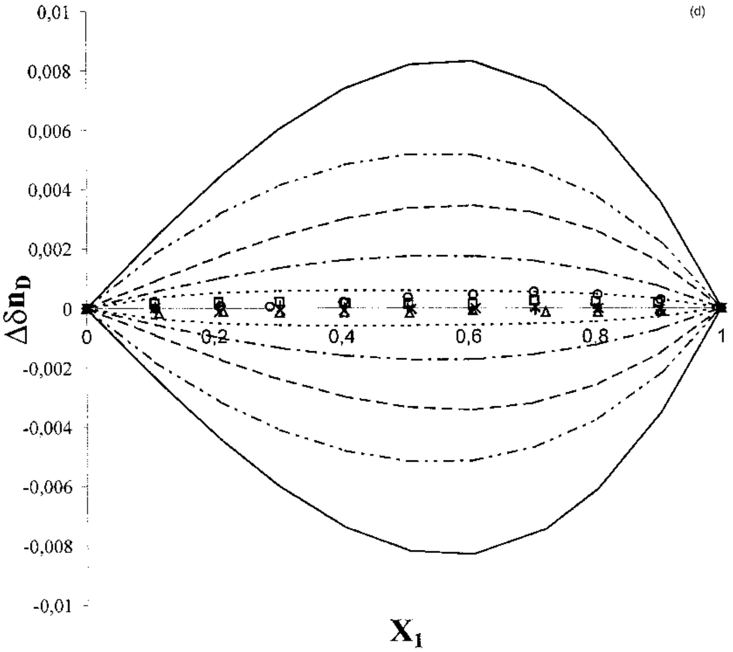

FIGURE 4 Continued.

where the symbols keep the meaning explained above. From Eq. (6), the corresponding limiting partial excess molar volumes should be determined by considering x_i rule for each case, such limiting values being dependent only on these correlation parameters. Figure 5(a,b) shows the trends of partial excess molar volumes with the corresponding molar fraction for the binary mixtures. It is worthwhile to point out the fast increasing of negative values of the partial magnitude for increasing chain length and composition of diluent. In Table IV, the values of limiting partial excess molar volumes at 298.15 K for the binary mixtures are enclosed. These values show the slight influence on the excess molar volumes of similar compounds into *n*-hexane environment, with slight expansion for *n*-heptane and decreasing contractive tendence as concentrations of *n*-hexane increase for the others.

3.3. Estimation of Derived Magnitudes

Due to the strong dependence of design and optimization of chemical processes on computer calculations, the availability of accurate, simple and tested methods, as well as, the corresponding necessary parameters is of increasing relevance. In this case, consideration was given to the Rackett equation of state [18,19] in order to analyze how accurate densities are predicted. Attending to these models, the density could be described as:

$$\rho = \left(\frac{MP_c}{RT_c}\right)\beta^{-[1+(1-T_r)^{2/7}]} \tag{7}$$

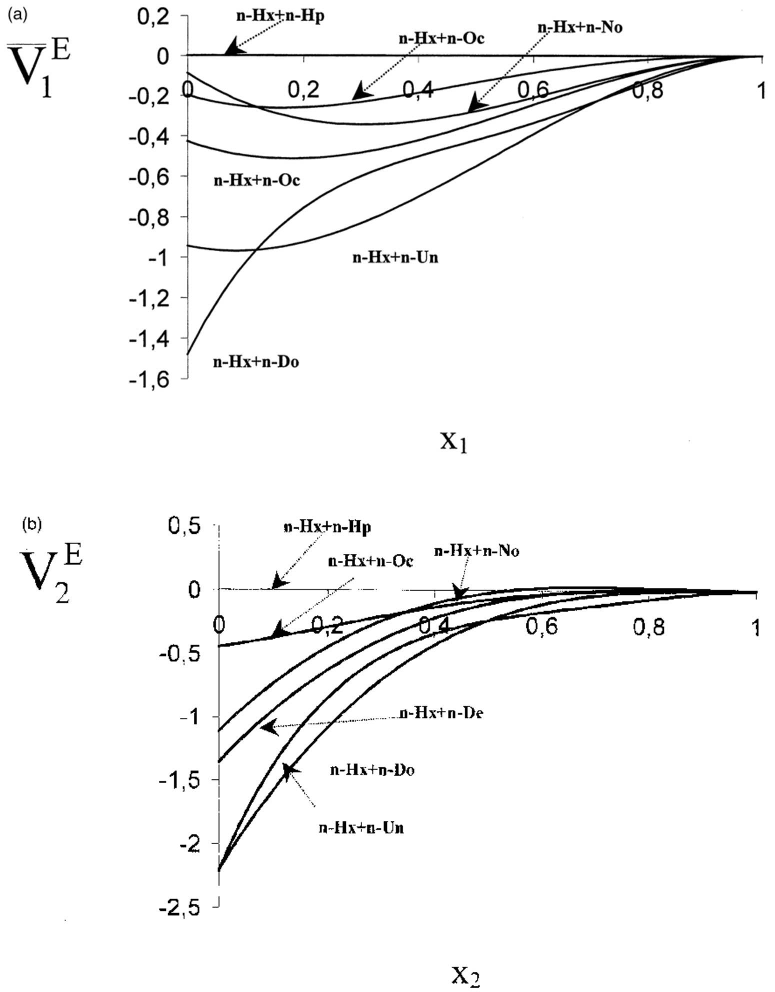

FIGURE 5 Partial excess molar volumes ($cm^3\,mol^{-1}$) of the binary systems. (a) $\overline{V}_1^E$ and (b) $\overline{V}_2^E$ at 298.15 K (*n*-Hp, *n*-heptane; *n*-Oc, *n*-octane; *n*-No, *n*-nonane; *n*-De, *n*-decane; *n*-Un, *n*-undecane; *n*-Do, *n*-dodecane).

where T_r is the reduced temperature for the mixture, T_c and P_c are the seudocritical mixing properties, and β is the compressibility factor or an acentric factor dependent parameter which varies attending to a molecular structure parameter [20]. The selected mixing rule to compute density was proposed by Kay (modified combination of Prausnitz–Gunn) [21,22]. In order to predict the mixing density, critical properties are required for each compound, open literature or estimative methods should be used. In Table V, open literature critical values are gathered [23] for the compounds enclosed in the studied mixtures. In Table VI, a comparison between the binary experimental and estimated densities is shown in terms of the root mean square deviations. Attending to these values, it was observed that Rackett and modified Rackett equation predict adequately for these binary mixtures, better results being showed with the latter equation.

TABLE IV Partial excess molar volumes at infinite dilution of the binary mixtures at 298.15 K

	$\overline{V}_1^{E,\infty}/(\mathrm{cm^3\,mol^{-1}})$	$\overline{V}_2^{E,\infty}/(\mathrm{cm^3\,mol^{-1}})$
n-Hexane + *n*-heptane	0.0019	0.0021
n-Hexane + *n*-octane	−0.1970	−0.4446
n-Hexane + *n*-nonane	−0.0877	−1.1127
n-Hexane + *n*-decane	−0.4266	−1.3562
n-Hexane + *n*-undecane	−0.9435	−2.2018
n-Hexane + *n*-dodecane	−1.4799	−2.2108

TABLE V Open literature critical values for the compounds enclosed into binary mixtures

Compound	P_c (atm)	T_c (K)	Z_c	ω
n-Hexane	23.73	507.43	0.264	0.3047
n-Heptane	27.00	540.26	0.263	0.3494
n-Octane	24.54	568.83	0.259	0.3962
n-Nonane	22.75	595.65	0.255	0.4368
n-Decane	20.95	618.45	0.249	0.4842
n-Undecane	19.40	638.76	0.243	0.5362
n-Dodecane	18.00	658.20	0.238	0.5752

TABLE VI Root mean square deviations for estimated density by Rackett (*R*) or modified Rackett (*mR*) with respect to experimental density for the binary mixtures

	R	*mR*
n-Hexane + *n*-heptane	0.0159	0.0094
n-Hexane + *n*-octane	0.0153	0.0052
n-Hexane + *n*-nonane	0.0210	0.0335
n-Hexane + *n*-decane	0.0256	0.0140
n-Hexane + *n*-undecane	0.0614	0.0294
n-Hexane + *n*-dodecane	0.0687	0.0080

TABLE VII Root mean square deviations for estimation of refractive index on mixing (Lorentz–Lorenz rule) with respect to experimental refractive indices for the binary mixtures

n-Hexane + *n*-heptane	0.00017
n-Hexane + *n*-octane	0.00031
n-Hexane + *n*-nonane	0.00054
n-Hexane + *n*-decane	0.00077
n-Hexane + *n*-undecane	0.00110
n-Hexane + *n*-dodecane	0.00800

Although good results are obtained for density, no accurate data were obtained for the excess molar volumes by estimated densities.

In what is referred to the refractive indices on mixing, the experimental data were compared with the results by the mixing rule proposed by Lorentz–Lorenz [24]. In Table VII, the root mean square deviations for the binary mixtures are enclosed, where the higher values were obtained in those mixtures of the highest nonideality.

TABLE VIII Root mean square deviations for estimation of isentropic compressibilities (TPa^{-1}) obtained by applying the methods of Jacobson (FLT) and Schaffs–Nutsch-kuhnkies (CFT) with respect to experimental isentropic compressibilities for the binary mixtures

	Jacobson (FLT)	*Schaffs–Nutsch-kuhnkies (CFT)*
n-Hexane + *n*-heptane	16.45	0.38
n-Hexane + *n*-octane	14.53	0.13
n-Hexane + *n*-nonane	15.52	0.96
n-Hexane + *n*-decane	14.34	0.47
n-Hexane + *n*-undecane	13.26	0.04
n-Hexane + *n*-dodecane	12.43	0.40

The Jacobson (Free Length Theory) [25] and Schaffs–Nutsch-kuhnkies (Collision Factor Theory) [26–28] methods were applied to the isentropic compressibilities estimation. In Table VIII, the root mean square deviations are gathered. The application of the Collision Factor Theory (CFT) presents the lowest deviations for predicting the isentropic compressibilities, only a qualitative description being obtained for the other theory.

4. RESULTS AND CONCLUSIONS

In earlier articles [29–34], we reported the volumetric and phase equilibria behavior of different alkanes related to the separation of the azeotropic mixture acetone + methanol by heterogeneous extractive distillation. The promising role of such type of compounds leads us to investigate the cosolvent effect of different *n*-alkanes as entrainers for this process, in order to obtain as benefits, an adequate quaternary phase splitting and residual topology [35]. In this work, the densities, refractive index and speed of sound have been measured at 298.15 K for different *n*-alkane mixtures. Derived properties were calculated from the experimental measurements, the data being correlated by polynomial expressions which fitted the data well. Generally, the derived data reported in this study on the systems *n*-hexane + (*n*-heptane, *n*-octane, *n*-nonane, *n*-decane, *n*-undecane, or *n*-dodecane) at 298.15 K and atmospheric pressure are only in desagreement with those reported earlier by other authors for the system *n*-hexane + *n*-heptane, due to their low values of derived properties. Not surprisingly, the systems exhibited nearly ideal behavior, but with an increasing contractive tendence as the aliphatic chain rises.

It is well known that when nonpolar compounds are mixing, slight variations in the intermolecular interactions take place. The new specific dispersive interactions that appear should be suitably measured by combining volumetric or calorimetric techniques. Usually, these kind of mixtures show a moderate nonideal behavior, which is severely conditioned by the difference in molecular volume between the *n*-alkanes. In this case, the steric hindrance is the most important factor in mixing thermodynamics. This fact is noted by a contractive trend in mixtures, except for cases of dilution of *n*-hexane in *n*-heptane environment, where a slight expansive effect is reflected.

In the mixture acetone + methanol + *n*-alkanes, carbonyl/hydroxil polar functional groups and inert methylene groups are contained, the functional dependence could be expressed attending to the following factors; first, the aliphatic chain of the separation agents leads to an expansive trend at low acetone molar fraction, a phase-splitting being inducted. The self-association and crossed H-bonds are strong enough to package the mixture at low entrainer concentrations, while at high concentrations, only a mixing expansion being obtained. An adequate residual topology is obtained throughout the whole mixture if the molecules of entrainers are C_{10} or greater [36], or as a result of this study, a combination of C_6 and C_8–C_{12} solvents. This trend is explained due to an intense repulsion with methanol due to the bond potency of the hydroxil of this compound, and its virtually zero steric hindrance.

The interaction of possible cosolvents herein studied tally with the trend observed in the above indicated literature, this tendence being of interest in order to separate acetone and methanol by means of an adequate vapor–liquid equilibria topology.

This fact is clearly shown in Fig. 5(a,b), where the curves for the partial excess molar volumes rise through the entire composition range. The comparison of our experimental data with earlier contributions reveals high deviations for the lighest mixtures, pointing out better accuracies and thermodynamic coherence for these mixtures. The experimental measurements are closely related to changes in the solvent layer around the *n*-hexane molecules; the solvation layer is progressively dissolved, as concentration of solvent increases the weak dispersive interactions among *n*-hexane molecules being replaced by stronger interactions among *n*-hexane and the solvent molecules. A minimum was reached at equimolar compositions for the mixtures C_6–C_8 to C_{12}. The strongest contracting trend was observed for *n*-hexane + *n*-dodecane mixture.

These types of interactions among heavy aliphatic solvents, acetone and methanol molecules provide promising expectations. These kind of entrainers show an important capability to disrupt alcohol–ketone interactions, while an adequate vapor–liquid equilibria topology is performed (only one minimum azeotrope in the problem multicomponent mixture), which highlights the potency of these agents for separation processes, that implies simple sequences and low costs for application in extractive or modified distillation procedures. Currently, our work is to be focused on the application of aliphatic heavy compounds with splitting induction into the acetone + methanol mixture, in order to reinforce the observed behavior for these chemicals, as well as, phase equilibria studies on these mixtures.

References

[1] C. Gonzalez, M. Iglesias, J. Lanz and J.M. Resa (1999). *Thermochimica Acta*, **328**, 277.
[2] M. Iglesias, B. Orge, G. Marino and J. Tojo (1999). *J. Chem. Eng. Data*, **44**, 661.
[3] M.J. Fontao and M. Iglesias (2000). *Phys. Chem. Liq.*, **38**, 623.
[4] A. Touriño, M. Iglesias and G. Marino (2002a). *J. Sol. Chem.*, **31**, 793.
[5] *TRC Thermodynamic Tables* (1994). Thermodynamic Research Center. Texas A&M University: College Station, TX.
[6] T.M. Aminabhavi, V.B. Patil, M.I. Aralaguppi and H.T.S. Phayde (1996). *J. Chem. Eng. Data*, **41**, 521.
[7] L. Hnedkovsky and I. Cibulka (1993). *Int. DATA Ser., Sel. Data Mixtures. Ser. A.*, **21**(2), 167.
[8] N.V. Sastry and M.K. Valand (1996). *J. Chem. Eng. Data*, **41**, 1421.
[9] T.M. Aminabhavi and B.P. Virupaxagouda (1997). *J. Chem. Eng. Data*, **42**, 641.
[10] M.I. Aralaguppi, C.V. Jadar and T.M. Aminabhavi (1999). *J. Chem. Eng. Data*, **44**, 435.
[11] E. Junquera, E. Aicart and G. Tardajos (1989). *J. Chem. Thermodyn.*, **21**, 1223.
[12] O. Redlich and A.T. Kister (1948). *Ind. Eng. Chem.*, **40**, 345.
[13] P. Bevington (1969). *Data Reduction and Error Analysis for the Physical Sciences*. McGraw-Hill, New York.
[14] J.R. Goates, J.B. Ott and R.B. Grigg (1981). *J. Chem. Thermodyn.*, **13**, 907.

[15] J.L.E. Chevalier, P.J. Petrino and Y.H. Gaston-Bonhomme (1990). *J. Chem. Eng. Data*, **35**, 206.
[16] A. Aucejo, M.C. Burguet, R. Muñoz and J.L. Marques (1995). *J. Chem. Eng. Data*, **40**, 141.
[17] A. Touriño, M. Hervello, V. Moreno, M. Iglesias and G. Marino (2002). *J. Chem. Thermodyn.*, (submmitted for publication).
[18] H.G. Rackett (1970). *J. Chem. Eng. Data*, **15**, 514
[19] C.F. Spencer and R.P. Danner (1972). *J. Chem. Eng. Data*, **17**, 236.
[20] R.C. Reid, J.M. Prausnitz and B.E. Poling (1988). *The Properties of Gases and Liquids*, 4th Edn. McGraw-Hill. Singapore.
[21] W.B. Kay (1936). *Ind. Eng. Chem.*, **28**, 1014.
[22] J.M. Prausnitz and R.D. Gunn (1958). *AIChE J.*, **4**, 430.
[23] J.A. Riddick, W.B. Bunger and T.K. Sakano (1986). *Organic Solvents*, 4th Edn. Wiley-Interscience, New York.
[24] M. Iglesias, B. Orge and J. Tojo (1996). *Fluid Phase Eq.*, **126**, 203.
[25] B. Jacobson (1952). *Acta Chemica Scandinavica*, **6**, 1485.
[26] R. Nutsch-kuhnkies (1965). *Acustica*, **15**, 383.
[27] W. Schaffs (1975a). *Z. Phys.*, **114**, 110.
[28] W. Schaffs (1975b). *Z. Phys.*, **115**, 69.
[29] G. Marino, M. Iglesias, B. Orge and J. Tojo (2000a). *J. Chem. Thermodyn.*, **32**, 483.
[30] G. Marino, B. Orge, M. Iglesias and J. Tojo (2000b). *J. Chem. Eng. Data*, **45**, 457.
[31] M. Iglesias, B. Orge, G. Marino, M.M. Piñeiro. and J. Tojo (2001). *J. Solution Chemistry*, **30**, 135.
[32] G. Marino, M.M. Piñeiro, M. Iglesias, B. Orge and J. Tojo (2001). *J. Chem. Eng. Data*, **46**, 728.
[33] A. Touriño, L.M. Casás, G. Marino, M. Iglesias, B. Orge and J. Tojo (2003). *Fluid Phase Eq.*, **206**, 61.
[34] L.M. Casás, A. Touriño, G. Marino, M. Iglesias, B. Orge and J. Tojo (2001). *J. Chem. Eng. Data*, **47**, 887.
[35] J. Tojo and M. Iglesias (1995). *Afinidad*, **LII**, 78.
[36] G. Marino (2001). PhD. Thesis, Vigo University.